

Sound velocity and elasticity of tetragonal lysozyme crystals by Brillouin spectroscopy

S. Speziale^a, F. Jiang^{a,b}, C.L. Caylor^b, S. Kriminski^b, C-S. Zha^c, R.E. Thorne^b, T.S.
Duffy^a,

^aDepartment of Geosciences, Princeton University, Princeton, NJ 08544 USA

^bLaboratory of Atomic and Solid State Physics, Cornell University, Ithaca, NY 14853
USA

^cCornell High-Energy Synchrotron Source, Ithaca, NY 14853 USA

Abstract

Quasi-longitudinal sound velocities and the second-order elastic moduli of tetragonal hen egg-white lysozyme crystals were determined as a function of relative humidity by Brillouin scattering. In hydrated crystals the measured sound velocities in the (110) plane vary between 2.12 ± 0.03 km/s along the [001] direction and 2.31 ± 0.08 km/s along the $[1\bar{1}0]$ direction. Dehydration from 98% to 79% relative humidity increases the sound velocities and decreases the velocity anisotropy in (110) from 8.2% to 2.8%. A discontinuity in velocity and an inversion of the anisotropy is observed with increasing dehydration providing support for the existence of a structural transition below 88% relative humidity. At equilibrium hydration (98% relative humidity) the longitudinal moduli: $C_{11} + C_{12} + 2C_{66} = 12.81 \pm 0.08$ GPa, $C_{11} = 5.49 \pm 0.03$ GPa, and $C_{33} = 5.48 \pm 0.05$ GPa were directly determined. Inversion of the measured sound velocities in the (110) plane constrains the combination $C_{44} + 1/2C_{13}$ to 2.99 ± 0.05 GPa. Further constraints on the elastic tensor are obtained by combining the Brillouin quasi-longitudinal results with axial compressibilities determined from high-pressure x-ray

diffraction. We constrain the adiabatic bulk modulus to the range 2.8 - 5.1 GPa. Brillouin scattering is a promising non-contact method to investigate the elastic tensor of protein crystals.

1. Introduction

The biological activity of proteins is closely connected to their conformational flexibility. The interplay between chemical properties, mechanical properties and thermal fluctuations gives rise to structural fluctuations and conformation changes that play an essential role in ligand binding, catalysis, and other protein functions in living cells (Morozov and Morozova, 1993). In addition, the understanding of the relationship between chemical structure and mechanical properties in proteins is a promising frontier of biotechnology and material sciences (Gosline et al., 2002). The mechanical properties of proteins can be probed by measuring the elastic tensor of protein crystals (Morozov and Morozova, 1993). Crystal elasticity is determined by the anisotropic elasticity of the individual molecules and of the crystal contacts between molecules. Studies on a wide array of organic and inorganic materials demonstrate that the elastic tensor and associated damping constants can provide detailed information about both static structure and dynamical processes (e.g. Patterson, 1977; Krüger et al., 1986; Tao et al., 1988). The elastic tensor also gives information about crystal properties such as the energetics of cracks, dislocations, vacancies and other defects that determine crystal mosaicity, an important parameter in molecular structure determination by x-ray crystallography.

Protein crystal elasticity has been explored using mechanical resonance techniques (Morozov and Morozova, 1981; Gevorkyan and Morozov, 1983; Morozov and

Morozova, 1986; Morozov et al., 1988; Morozov and Morozova, 1993), ultrasonic techniques (Edwards et al., 1990; Tachibana et al., 2000), and X-ray diffraction under hydrostatic pressure (Kundrot and Richards, 1987; Katrusiak et al., 1996; Fourme et al., 2001). The existing results from all of these techniques are fragmentary. Both ultrasound and resonance measurements in crystals are extremely demanding in terms of sample size and preparation. Extensive sample manipulations such as gluing, cutting and crosslinking can modify crystal properties (Morozov and Morozova, 1981; Edwards et al., 1990). Ultrasound measurements require crystals a few millimeters thick, limiting their applicability to the handful of proteins that yield crystals of such size.

Brillouin spectroscopy is a non-contact method that has the potential to give a more complete picture of protein crystal elasticity. It allows direct measurement of the sound velocity along general directions in a transparent medium and hence the determination of the elastic constant tensor of anisotropic materials. Brillouin spectroscopy has been widely used for the study of inorganic crystals (Zha et al., 1993; Sinogeikin and Bass, 2000), polymers (Mitsui and Iio, 1980; Krüger, 1989) and biological materials (Cusack and Miller, 1979; Vaughan and Randall, 1980; Hakim et al., 1984; Lee et al., 1993).

Here we report results of the first extensive Brillouin scattering study of protein crystal elasticity. We show that Brillouin scattering can be used to obtain detailed information about the elastic constant tensor using sub-millimeter size protein crystals maintained in their growth environment. Our initial focus is on tetragonal hen-egg-white lysozyme crystals and on the effects of hydration state. Some preliminary results have been published elsewhere (Caylor et al., 2001).

2. Samples and Experimental Methods

Tetragonal hen egg-white lysozyme crystals were grown at 21°C in hanging and sitting drops and in agarose gels (0.1% w/v), using solutions consisting of 40-60 mg/ml lysozyme (Seikagaku, 6x recrystallized) and 0.5M NaCl in 50mM acetate buffer at pH = 4.5. All crystals had well developed {110} and {101} faces, and gel grown crystals had nearly ideal habits. The equilibrium relative humidity corresponding to the growth conditions was 98%.

Crystals were dehydrated to different r.h. by equilibration with vapors of saturated salt solutions of KNO₃ (93% relative humidity), KCl (86%), KBr (83%), (NH₄)₂SO₄ (79%), NaCl (75%) and CuCl₂ (67%) (Rockland, 1960). X-ray topography and X-ray diffraction peak shape analysis (Dobrianov et al., 2000) show evidence of fine scale heterogeneities and dislocations in tetragonal lysozyme crystals dehydrated below 88% r.h. However, we did not observe any evidence of Brillouin signal degradation even in highly dehydrated crystals.

Using Brillouin scattering, acoustic velocities can be determined in a transparent medium from the frequency shift of laser light inelastically scattered by thermal vibrations. For an optically isotropic medium conservation of energy and momentum require that the frequency of the scattered light be shifted from that of the incident light by (Brillouin, 1922):

$$\Delta\omega = \pm 2 v n k_0 \sin(\theta/2), \quad (1)$$

where v is the phonon velocity in the measured direction, n is the refractive index of the scattering medium, k_0 is the wave vector of the incident light, and θ is the angle between the incident and scattered wave vectors. Three Brillouin peaks will in general be

produced by the three polarizations (quasi-longitudinal, and two quasi-transverse) of the scattering phonon along a general direction in crystalline solids. Due to its extremely low birefringence ($\Delta n = 0.005$; Cervelle et al., 1974), tetragonal lysozyme can be considered as an optically isotropic medium allowing equation (1) to be used in the analysis of the Brillouin spectra.

Brillouin scattering is performed using standard scattering geometries characterized by different angles between the directions of the incident and scattered light outside the sample that are shown in Figure 1(b-d). These geometries prevent overlap of sample scattering with the unshifted incident light and can enhance peak intensities by exploiting selection rules imposed by the elasto-optic coupling in the examined material (e.g. Cummins and Schoen, 1972).

The elastic tensor of tetragonal lysozyme (Laue group 4/mmm) has six unique non-zero elements (written in contracted notation as: C_{11} , C_{12} , C_{13} , C_{33} , C_{44} , C_{66}). The relationship between velocity and polarization of the phonon and the elastic properties of the scattering medium are expressed by Christoffel's equation (Auld, 1973):

$$(C_{iklm}l_kl_m - \rho v^2 \delta_{il}) u_l = 0, \quad (2)$$

where C_{iklm} are the elastic constants, l_k and l_m are the direction cosines of the phonon, and u_l is the local displacement vector, ρ is the density of the material, δ_{il} is the Kronecker delta. Equation (2) is a set of three homogeneous equations, which have non-trivial solutions only if

$$| C_{iklm}l_kl_m - \rho v^2 \delta_{il} | = 0. \quad (3)$$

This is a cubic equation in ρv^2 with three real positive roots.

A vertically polarized neodymium vanadate laser ($\lambda = 532.15$ nm) operated at 1.59 W and filtered to 1.59 mW was used as an excitation source. X-ray topography and diffraction resolution measurements performed at the Cornell High-Energy Synchrotron Source (CHESS) on crystals after extended laser illumination verified that these small powers caused no heating damage. Brillouin spectra were acquired using a six-pass Sandercock tandem Fabry-Perot interferometer (Lindsay et al., 1981) and a solid-state photon detector with 70% quantum efficiency. Experiments were performed with and without polarization control in the incident and scattered light path. A diagram of the setup of the Brillouin system used in this study is outlined in Figure 2. Selected crystals were mounted in square cross-section capillaries or sandwiched between parallel glass slides (Figure 1a). The typical size of the analyzed crystals was $\cong 400 \times 500 \times 100$ μm but Brillouin signal was obtained from crystals as small as $\cong 200 \times 300 \times 60$ μm .

Sound velocities were measured in the 90A forward scattering geometry (Figure 1c) along 10 to 18 directions in the (110) plane in crystals at 98%, 79% and 67% r.h. Sound velocities in the [110] and [001] directions were measured using the 90A and 90R scattering geometry (Figure 1d) in crystals at 93% and 86% r.h. (in 90A scattering geometry we actually measured the velocity along $[1\bar{1}0]$, which is physically equivalent to [110] due to the tetragonal symmetry). Sound velocities along [110] were measured in the 180 scattering geometry (Figure 1b) in crystals at 98% r.h. Measurement of sound velocity along the [100] direction were performed in the 90N scattering geometry (Figure 1e).

3. Results

In all the experiments only one of the three expected acoustic modes was detected. To identify this mode, we measured the Brillouin shift along the [110] and [001] directions controlling the polarization of the incident and scattered light. A half waveplate was used to rotate the polarization of the incident light, and polarizer and analyzer with high extinction ratio were inserted in the incident and scattered light paths respectively. The Brillouin scattered light intensity, I , can be expressed as (Cummins and Shoen, 1972):

$$I(\omega) \propto \{\mathbf{e}_s \cdot [\mathbf{T}_{ij}] \cdot \mathbf{e}_i\}^2, \quad (4)$$

where \mathbf{e}_s and \mathbf{e}_i are unit vectors in the direction of the polarization of the scattered and incident light \mathbf{T}_{ij} is the Brillouin scattering tensor component, which is related to the elasto-optic coupling tensor. The observed extinction of the Brillouin features in cross-polarized light confirms that the observed acoustic mode has a pure longitudinal polarization in the [110] and [001] directions and a quasi-longitudinal character in the intermediate directions. The absence of transverse modes may be due to the low efficiency of the elasto-optic coupling in the examined crystal directions, or to low transverse velocities that cause the corresponding peaks to be obscured by the tails of the elastic peak.

A typical spectrum, collected from a crystal at 98% r.h. is shown in Figure 3. Comparison of the frequency shift measured in the [110] direction in backscattering (180), forward symmetric (90A) and reflected symmetric geometry (90R) yields a refractive index of 1.51 ± 0.07 in good agreement with the value of 1.56 ± 0.01 obtained by oil immersion and with the value reported by Cervelle et al. (1974) of 1.538-1.575.

The observed acoustic velocities along the (110) plane of tetragonal lysozyme reveal significant velocity anisotropy, expressed as the absolute value of the difference between the velocity measured along the [110] and [001] directions (Figure 4). The anisotropy decreases with increasing dehydration from 0.2 km/s at 98% r.h. to 0.09 km/s at 67% r.h. The character of the anisotropy changes between between 93% and 86% r.h., as indicated by the variation of acoustic mode velocity with crystallographic direction and by a discontinuity in the general trend of increasing acoustic velocity with the degree of dehydration (Figure 4).

4. Discussion

In the [110] direction, Christoffel's equation for the tetragonal system can be factored. The solution for the quasi-longitudinal acoustic velocity has the form (e.g. Auld, 1973):

$$v_{[110]L} = \sqrt{\frac{C_{11} + C_{12} + 2C_{66}}{2\rho}}, \quad (5)$$

where ρ is the density of crystalline lysozyme (taken from the isothermal dehydration data from Gevorkyan and Morozov, 1983). The velocity measured along the [001] direction allows us to directly determine the constant C_{33} from (Auld, 1973):

$$v_{[001]L} = \sqrt{\frac{C_{33}}{\rho}} \quad (6)$$

The effective elastic constants along these two directions show a discontinuity as a function of degree of dehydration in the 93 – 86% r.h. range (Figure 5), in agreement with the direct sound velocity measurements.

The velocities of the quasi-longitudinal acoustic mode along the [110] and [001] directions at 98% r.h. are 2.31 ± 0.04 km/s and 2.12 ± 0.03 km/s respectively. Additional measurements along the [100] direction resulted in a velocity of 2.13 ± 0.01 km/s. These velocities correspond to values for the longitudinal modulus $M_{L[110]} = C_{11} + C_{12} + 2C_{66} = 12.81 \pm 0.08$ GPa, $M_{L[001]} = C_{33} = 5.48 \pm 0.05$ GPa, and $M_{L[100]} = C_{11} = 5.49 \pm 0.03$ GPa. The longitudinal acoustic velocity along [110] and the effective stiffness $M_{L[110]}$ is larger than the value determined by ultrasonic measurements performed by Tachibana et al. (2000, 2002) (Table 1). The difference of the measured velocities (25%) and, as a consequence, of the longitudinal modulus (60%) are much larger than the uncertainties.

The dependence of the measured acoustic velocity on the phonon direction (Figure 6) at 98% r.h. is anisotropic. The maximum measured velocity along [110] and the minimum velocity along [001] differ by 0.20 km/s (8.2%). Bounds to the value of Young's modulus, E , can be estimated assuming elastic isotropy, as in Tachibana et al. (2000), using (e.g. Auld, 1973):

$$E = \frac{(1+\sigma) \cdot (1-2\sigma) \cdot M_L}{(1-\sigma)} \quad (7)$$

where M_L is the longitudinal modulus, and σ is Poisson's ratio.

Using the longitudinal moduli along [100], [001] and [110] and fixing Poisson's ratio to 0.33, as observed in many polymers, the two "bounds" to the value of the isotropic Young's modulus from data in the [110] and [001] directions are 4.32 ± 0.03 and 3.69 ± 0.02 GPa (Table 1). These values are higher than the dynamic moduli determined with the microreed method (Morozov et al., 1988) and the isotropic value from ultrasonic measurements (Tachibana et al., 2000) and suggest a frequency dependence of Young's modulus (Figure 7).

The measurements performed in this study show that dehydration increases the sound velocity in tetragonal lysozyme crystals, consistent with previous measurements of elastic properties of dehydrated triclinic lysozyme crystals (Morozov and Morozova, 1981). Dehydration also decreases the overall velocity anisotropy along the (110) plane from 8.2% at 98% r.h. to 2.8% at 79% r.h. to 2% at 67% r.h. (Figure 6). The [110] direction is the fastest direction at elevated r.h., but the anisotropy inverts below 93% r.h., and [001] becomes the fastest direction. This suggests an anisotropic sensitivity to dehydration with a preferential stiffening along the *c* crystallographic axis, possibly related to the more than 10% observed contraction of the *c*-axis lattice parameter with decreasing r.h. (Dobrianov et al., 2001).

The longitudinal acoustic velocities along [110] and [001] directions as a function of dehydration show a discontinuity in the range from 93% to 86% r.h. (Figure 4). This is in agreement with X-ray diffraction evidence for a structural phase transition in the same humidity range (Salunke et al., 1985, Dobrianov et al., 2001). Sound velocity discontinuities as a function of relative humidity have been interpreted as a phase transition in other organic systems (Lee et al., 1993).

After correction for instrumental broadening, we calculated the normalized attenuation of the quasi-longitudinal phonons in the [110] and [001] directions (e.g. Lee et al., 1993):

$$\alpha\lambda_S = 2\pi \Gamma_{1/2}/\Delta\nu_B, \quad (8)$$

where α is the phonon's energy decay constant, λ_S is the phonon wavelength, $\Gamma_{1/2}$ is the half width at half maximum of the Brillouin peak, and $\Delta\nu_B$ is the Brillouin frequency shift.

The phonon attenuation decreases with dehydration, and it does not show any discontinuity in the 93 – 86% r.h. range (Figure 8). The value of the phonon attenuation for both the [001] and [110] directions ranges between 0.3 and 0.9, and it is comparable to hypersonic attenuation obtained for plastic crystalline organic solids such as DL-camphene, norbornylene, succinonitrile (0.4 – 0.5; Boyer et al., 1971; Folland et al., 1975; Bird et al., 1975) and for amorphous organic solids as polymethyl - acrylate and polypropylene glycol (0.5 – 0.7; Huang et al., 1971; Huang and Wang, 1975), although other factors including static disorder and the effect of coupling with the relaxation mode of the hydration shell (Tao et al., 1988; Lee et al., 1993) could contribute to the observed peak width. We plan to investigate the details of hypersonic attenuation in lysozyme and its dependence on dehydration in a future study.

5. Additional constraints on the elastic tensor of lysozyme

Christoffel's equation (equation 2) can be factored for the (110) plane in the tetragonal system. The phonon velocity is (Fedorov, 1958; Winternheimer and McCurdy, 1978):

$$v_1 = \sqrt{\frac{A_1 \sin^2 \theta}{2\rho} + \frac{C_{44} \cos^2 \theta}{\rho}}, \quad (9)$$

$$v_{0,2} = \sqrt{\frac{(A_2 + C_{44}) \sin^2 \theta + A_3 \cos^2 \theta \pm \left\{ \left[(A_2 - C_{44}) \sin^2 \theta - A_4 \cos^2 \theta \right]^2 + (2A_5 \sin \theta \cos \theta)^2 \right\}^{1/2}}{2\rho}}, \quad (10)$$

where θ is the angular direction of the phonon wave vector with respect to the [001] direction, ρ is the crystal density, and

$$A_1 = C_{11} - C_{12},$$

$$A_2 = \frac{1}{2}(C_{11} + C_{12}) + C_{66},$$

$$A_3 = C_{33} + C_{44},$$

$$A_4 = C_{33} - C_{44},$$

$$A_5 = C_{13} + C_{44}.$$

Equation (9) gives velocities of the pure transverse acoustic mode, while equation (10) gives the velocities of the quasi-longitudinal and the quasi-transverse modes.

The longitudinal acoustic mode velocities measured along the (110) plane in crystals at 98%, 79% and 67% r.h. were fitted to the Christoffel's equation to obtain a subset of the second order elastic tensor. The absence of observed transverse acoustic phonon velocities restricts our ability to recover the complete elastic tensor (Castagnede et al., 1992), and allows us only to give constraints on the combination of C_{44} and C_{13} in addition to the combination $C_{11} + C_{12} + 2C_{66}$ and C_{33} . Additional constraints on the elastic constants derive from the strain energy stability requirement that the elastic tensor is positive definite, which for a tetragonal crystal translates into (Fedorov, 1958):

$$\begin{aligned} C_{11} - |C_{12}| &> 0, \\ (C_{11} + C_{12})C_{33} - 2C_{13}^2 &> 0, \\ C_{66} &> 0. \end{aligned} \tag{11}$$

The procedure to obtain the elastic constants consisted of two steps: a preliminary parameter search in elastic constant space, and a final nonlinear least-square inversion of the Christoffel's equation performed using the results of the parameter search as a starting model. The inversion routine was based on the Levenberg – Marquardt algorithm.

The same two-stage procedure was applied also to invert the velocity data for the lysozyme crystals at 98%, 79% and 67% r.h. The inversion of the longitudinal velocities allowed us to constrain the combination $C_{44} + 1/2 C_{13}$. The high linear correlation between these two constants is clearly visible Figure 9, which provides an illustration of the “goodness of fit” in the case of 98% r.h. for a wide range of C_{13} , C_{44} values when the other constants are fixed to the best model values. The best solutions are not distinguishable at the 70% confidence level at all the relative humidity conditions. The best-fit constants for the examined degrees of dehydration are reported in Table 2. The calculated and observed sound velocities are compared in Figure 7.

The fit results and the mechanical stability conditions allowed us to determine bounds to the values of some elastic moduli (Table 2). The calculated adiabatic bulk modulus, $K_S = - (dP/d\ln V)_S$, at 98% r.h. ranges between 0.18 and 5.0 GPa. Our result marginally overlaps the range of values of the bulk modulus of native proteins in solution and of lysozyme crystals (4 - 10 GPa; Kundrot and Richards, 1986; Katrusiak and Dauter, 1996; Kharakoz, 2000; Fourme et al., 2001).

In the case of 98% r.h. the direct measurement of the longitudinal acoustic velocity along the [100] direction allows us to fix the value of C_{11} to 5.49 ± 0.01 GPa. The values of the axial compressibilities determined from high-pressure diffraction (Kundrot and Richards, 1987; Fourme et al., 2001) can be used to provide additional constraints on the elastic constants and bulk modulus, if we neglect the difference between the isothermal and isentropic moduli. The logarithmic ratio of the axial compressibilities along the c and a axes (Nye, 1985) is:

$$\frac{\partial \ln c}{\partial \ln a} = \frac{a}{c} \frac{\partial c / \partial P}{\partial a / \partial P} = \frac{2s_{13} + s_{33}}{s_{11} + s_{12} + s_{13}} = \frac{C_{11} + C_{12} - 2C_{13}}{C_{33} - C_{13}}. \quad (12)$$

This quantity has the advantage that it is independent of systematic errors in the measured pressures.

Combining Brillouin scattering results, axial compressibilities from high-pressure x-ray diffraction by Fourme et al. (2001) (equation 12) and the constraints imposed by stability criteria (equations 11) we can constrain the value of all the constants for a fixed value of C_{44} between 0.4 and 1.4 GPa (limits fixed by the stability constraints). The range of allowed values of the individual constants and the stability criteria are shown in Figure 10a, the range of the values of Young's modulus and of selected aggregate elastic moduli are shown in Figure 10b. The bulk modulus can range between the values of 5.1 and 2.8 GPa. However, the value of the bulk modulus remains a factor of two below that obtained from static compression of tetragonal lysozyme (Kundrot and Richards, 1987; Fourme et al., 2001).

This discrepancy may in part be due to the difficulty of obtaining a reliable bulk modulus from volume – pressure data over a very limited range of compression. For instance, Fourme et al. (2001) used the ruby fluorescence pressure scale, which is primarily calibrated from measurements made at much higher pressures. While the precision of the ruby fluorescence measurements can be high, the accuracy of the pressure scale is not well established (Dzwolak et al., 2002). A small absolute inaccuracy, negligible at high pressure, can have a dramatic effect in the comparatively low pressure regimes covered by high-pressure protein crystallography. In addition, systematic errors can result from other factors such as temperature variations (0.02 GPa/K) and internal stresses in ruby grains. The use of equation (12) does not require knowledge of the pressure and thus is not subject to these limitations.

The combined constraints from Brillouin scattering and high-pressure x-ray diffraction measurements restrict the range of values of the shear modulus to 0.2 – 1.3 GPa (Figure 10b). The “isotropic” Poisson’s ratio is not well constrained, and it can range between the value of 0.48 (for $C_{44} = 0.4$ GPa) and 0.30 when $C_{44} = 1.4$ GPa. This wide range corresponds both to values common to rigid polymers, and to those of soft rubbers. It is interesting to notice that a value similar to the upper bound (0.47) was determined for crystals of ribonuclease-A and human haemoglobin (Edwards et al., 1990).

Upper and lower bounds to the values of Young’s moduli along the [110] and [001] directions (see for instance Nye, 1985, p. 145) are 0.8 and 0.7 GPa (lower bound) and 4.8 and 4.1 GPa (upper bound) respectively (Figure 9b, Table 3). The value of the two moduli is strongly constrained to 2.4 ± 0.5 GPa and 2.3 ± 0.4 GPa, respectively, when C_{44} is larger than 0.8 GPa. These values overlap the Young’s moduli calculated in the assumption of elastic isotropy and with Poisson’s ratio of 0.33 (Table 1) and confirm the existence of a frequency dependence of the elastic moduli (Figure 7). The average logarithmic frequency derivative, $\partial E/\partial \log v$, calculated combining the results of this study with the range of the available data from different techniques (see Figure 7), ranges between 0.2 and 0.4 GPa/decade over the range Hz to 10^9 Hz. This values are in good agreement with the available data of frequency dependence of the bulk modulus in polymers (0.04 – 0.5 GPa/decade; Lagakos et al., 1986), and indicates that protein crystals exhibit a viscoelastic response.

6. Conclusions

Brillouin scattering of tetragonal lysozyme along directions in the (110) plane allowed the direct determination of the acoustic velocity, the velocity anisotropy and their dependence on the degree of dehydration. The effect of dehydration is to increase the stiffness and to decrease the elastic anisotropy of tetragonal lysozyme. A change of the sign of the elastic anisotropy and a velocity discontinuity are observed at relative humidity in the range between 93% and 86% consistently with x-ray structural observations reported by Dobrianov et al. (2001).

The dependence of velocity on the scattering direction places constraints on the elastic tensor at equilibrium humidity and at various degree of dehydration. The inverted elastic moduli provide a more detailed picture of lysozyme elasticity than has been possible using other techniques.

Our results demonstrate that Brillouin spectroscopy is a powerful probe of elastic and structural properties of protein crystals. It is a non-destructive, non-contact technique, which can be applied to protein crystals of ordinary size. The direct determination of the elasticity tensor, when combined with structural data from X-ray crystallography, will allow a more detailed analysis and understanding of protein structure and dynamics.

Acknowledgements

This work was supported by NASA (NAG8-1357, NAG8-1831), NSF (EAR-9725395) and the David and Lucille Packard Foundation (to TSD). CHESS is supported by the NSF (DMR 9713424).

References

Auld, B., Acoustic fields in and waves in solids, vol 1, 423 pp., John Wiley and sons, New York, London, Sidney, Toronto, 1973.

Bird, M.J., A.M. Amorim da Costa, and G.J. Hills, Light scattering studies of molecular motion in DL – camphene, in Light scattering in solids, edited by M. Balkanski, R.C.C. Leite and S.P.S. Porto, pp. 727-731, John Wiley and Son, New York, Sidney, Toronto, 1975.

Brillouin, Diffusion de la lumiere et des rayons X par un corps transparent homogene: Influence de l'agitation thermique, L., Ann. Physique, 17, 88-122, 1922.

Boyer, L., R. Vacher, M. Adam, and L. Cecchi, Rayleigh and Brillouin scattering in Succinonitrile, in Light scattering in solids, edited by M. Balkanski, pp. 498-501, Flammarion Science, Paris, 1971.

Castagnede, B., A.G. Every, W. Sachse, Numerical simulation of the instabilities associated to the recovery of elastic constants of anisotropic solids from quasi-longitudinal velocities alone, C.R. Acad Sci. Paris, 314, Serie II, 865-871, 1992.

Caylor C., S. Speziale, S. Kriminski, T. Duffy, C-S Zha, R.E. Thorne, Measuring the elastic properties of protein crystals by Brillouin scattering, J. Crystal Growth, 232, 498-501, 2001.

Cervelle, B., F. Cesbron, and J. Berthou, Morphologie et proprietes optiques des cristaux de lysozyme de poule de type quadratique et orthorhombique, Acta Cryst., A30, 645-648, 1974.

- Cummins, H.Z., and P.E. Schoen, Linear scattering from thermal fluctuations, in *Laser Handbook*, edited by F.T. Arecchi and E.O. Schultz-Dubois, North Holland, pp. 1029-1076, 1972.
- Cusak, S., and A. Miller, Determination of the elastic constants of collagen by Brillouin light scattering, *J. Mol. Biol.*, 135, 39-51, 1979.
- Dobrianov, I., S. Kriminski, C.L. Caylor, S.G. Lemay, C. Kimmer, A. Kisselev, K.D. Finkelstein, and R.E. Thorne, Dynamic response of tetragonal lysozyme crystals to changes in relative humidity: implications for post-growth crystal treatments, *Acta Cryst.*, D57, 61-68, 2001.
- Dzwolak, W., M. Kato, and Y. Taniguchi, Fourier transform infrared spectroscopy in high-pressure studies on proteins, *Biochim. Biophys. Acta*, 1595, 131-144, 2002.
- Edwards, C., S.B. Palmer, P. Emsley, J.R. Helliwell, D. Glover, G.W. Harris, and D.S. Moss, Thermal motion in proteins estimated using laser-generated ultrasound and Young's modulus measurements, *Acta Cryst.*, A46, 315-320, 1990.
- Fedorov, F.I., *Theory of elastic waves in crystals*, Plenum, New York, 1958.
- Folland, R., D.A. Jakson, and S. Rajogopal, Measurement of the elastic constants in the hexagonal plastic crystal of norbornylene, in *Light scattering in solids*, edited by M. Balkanski, R.C.C. Leite and S.P.S. Porto, pp. 694-701, John Wiley and Son, New York, Sidney, Toronto, 1975.
- Fourme R., R. Kahn, M. Mezouar, E. Girard, C. Hoerentrup, T. Prange', and I. Ascone, High-pressure protein crystallography (HPPX): instrumentation, methodology and results on lysozyme crystals, *J. Synchrotron Rad.*, 8, 1149-1156, 2001.

Gevorkyan, S.G., and V.N. Morozov, Dependence of the hydration isotherm of lysozyme on the packing of the molecules in the solid phase, *Biophysics*, 28, 1002-1007, 1983.

Gosline, J., M. Lillie, E. Carrington, P. Guerrette, C. Ortlepp, and K. Savage, Elastic proteins: biological roles and mechanical properties, *Phil. Trans. R. Soc. Lond.*, B 357, 121-132, 2002.

Hakim, M.B., S.M. Lindsay, and J. Powell, The speed of sound in DNA, *Biopolymers*, 23, 1185-1192, 1984.

Huang, Y.Y., E.A. Friedmann, R.D. Andrews, and T.R. Hart, Brillouin scattering and molecular relaxation in polymethyl acrylate, in *Light scattering in solids*, edited by M. Balkanski, pp. 488-493, Flammarion Science, Paris, 1971.

Huang, Y.Y., and C.H. Wang, Brillouin, Rayleigh, and depolarized scattering studies of polypropylene glycol. I, *J. Chem. Phys.*, 62, 120-126, 1975.

Katrusiak, A., and Z. Dauter, Compressibility of lysozyme protein crystals by X-ray diffraction, *Acta Cryst.*, D52, 607-608, 1996.

Kharakoz D., Protein compressibility, dynamics, and pressure, *Biophys. Journal*, 79, 511-525, 2000.

Krüger, J.K., Brillouin spectroscopy and its application to polymers, in *Optical techniques to characterize polymer systems*, edited by H. Bässler, *Studies in Polymer Science*, vol. 5, pp.429-534, Elsevier Science, 1989.

Krüger, J.K., A. Marx, L. Peetz, R. Roberts, and H.-G. Unruh, Simultaneous determination of elastic and optical properties of polymers by high performance Brillouin spectroscopy using different scattering geometries, *Coll. & Polym. Sci.*, 264, 403-414, 1986.

- Kundrot, C.E., and F. Richards, Crystal structure of hen egg-white lysozyme at a hydrostatic pressure of 1000 atmospheres, *J. Mol. Biol.*, 193, 157-170, 1987.
- Lagakos, N., J. Jarzynski, J.H. Cole, and J.A. Bucaro, Immersion apparatus for ultrasonic measurements in polymers, *J. Acoustic. Soc. Am.*, 56, 1469-1477.
- Lee, S.A., M.R. Flowers, W.F. Oliver, A. Rupprecht. S.M. Lindsay, Brillouin-scattering of hyaluronic acid: Dynamic coupling with the water of hydration and phase transitions, *Phys. Rev. E*, 47, 667-683, 1993.
- Lindsay, S.M., M.W. Anderson, and J.R. Sandercock, Construction and alignment of a high performance multipass vernier tandem Fabry-Perot interferometer, *Rev. Sci. Instrum.*, 52, 1478-1486, 1981.
- Mitsui, T., and K. Iio, Brillouin scattering in organic molecular crystal: meta-nitrobenzene, *Jpn. J. Appl. Phys.*, 19, 2511-2512, 1980.
- Morozov, V.N., and T. Ya. Morozova, Viscoelastic properties of protein crystals: Triclinic crystals of hen egg white lysozyme in different conditions, *Biopolymers*, 20, 451-467, 1981.
- Morozov, V.N., T. Na. Morozova, G.S. Kachalova, and E.T. Myachin, Interpretation of water desorption isotherms of lysozyme, *Int. J. Biol. Macromol.*, 10, 329-336, 1988.
- Morozov, V.N., and T. Ya. Morozova, Thermal motion of whole protein molecules in protein solids, *J. Theor. Biol.*, 121, 73-88, 1986.
- Morozov, V.N., and T. Ya. Morozova, Elasticity of globular proteins. The relation between mechanics, thermodynamics and mobility, *J. Biomol. Struct. Dyn.* 11, 459-481, 1993.
- Nye, J.F., *Physical properties of crystals*, 329 pp., Clarendon Press, Oxford, 1985

Patterson, G.D., Brillouin scattering and hypersonic relaxation in amorphous polymers, *J. Macromol. Sci.-Phys.*, B13, 647-664, 1977.

Rockland, J.T., Saturated salt solutions for static control of relative humidity between 5 degrees C and 40 degrees C, *Anal. Chem.*, 32, 1375-1376, 1960.

Salunke, D.M., B. Veerapandian, R. Kodandapani, and M. Vijayan, Water Mediated Transformations in Protein Crystals, *Acta Cryst.* B41, 431-436, 1985.

Tachibana, M., K. Kojima, R. Ikuyama, Y. Kobayashi, and M. Ataka, Sound velocity and dynamic elastic constants of ysozyme single crystals, *Chemical Physics Letters*, 332, 259-264, 2000.

Tachibana, M., K. Kojima, R. Ikuyama, Y. Kobayashi, and M. Ataka, Erratum to: 'Sound velocity and dynamic elastic constants of ysozyme single crystals', *Chemical Physics Letters*, 354, 360, 2002.

Tao, N.J., S.M. Lindsay, and A. Rupprecht, Dynamic coupling between DNA and its primary hydration shell studied by Brillouin scattering, *Biopolymers*, 27, 1655-1671, 1988.

Vaughan, J.M., and J.T. Randall, Brillouin-scattering, density and elastic properties of the lens and cornea of the eye, *Nature*, 284, 489-491, 1980.

Winternheimer, C.G., and A.K. McCurdy, Phonon focusing and phonon conduction in orthorhombic and tetragonal crystals in the boundary-scattering regime, *Phys. Rev. B*, 18, 12, 6576-6605, 1978.

Yeganeh-Haeri, A., D.J. Weidner, and J.B. Parise, Elasticity of α -cristobalite: A silicon dioxide with a negative Poisson's ratio. *Science*, 257 650-652, 1992.

Zha, C.-S., T.S. Duffy, H.-K. Mao, and R.J. Hemley, Elasticity of hydrogen to 24 GPa from single-crystal Brillouin scattering and synchrotron x-ray diffraction, *Phys. Rev. B*, 48, 9246-9255, 1993.

Table 1. Measured dynamic and static elastic moduli of tetragonal hen egg-white lysozyme

Technique	Longitudinal Modulus		Bulk Modulus	Young Modulus	
	$M_{L[110]}$ (GPa)	$M_{L[001]}$ (GPa)	K (GPa)	$E_{[110]}$ (GPa)	$E_{[001]}$ (GPa)
Brillouin – This study (dynamic modulus)	12.81 ^a -13.1 ^b	5.48 ^a -13.7 ^b		4.32 ^{a*}	3.69 ^{a*}
X-Ray diffraction (static modulus)			4-10 ¹		
Resonance method (dynamic modulus)					1.0 ^{2a} -8.0 ^{2c}
Microreed bending (static modulus)				0.18 ^{2a} -2.3 ^{2c‡}	
Ultrasonic pulse-echo (dynamic modulus)	7.99 ³			2.7 ^{3*}	

$$M_{L[110]} = C_{11} + C_{12} + 2C_{66}; M_{L[001]} = C_{33}$$

^a 98% relative humidity.

^b 67% relative humidity.

^c 0.01% relative humidity.

[‡] Average of the values for [001], [1 $\bar{1}$ 0], [100].

¹ Kundrot and Richards (1987), Kharakov (2000), Fourme (2001) 98% relative humidity.

² Morozov et al. (1988), 98 to 0.01% relative humidity.

³ Tachibana et al. (2000, 2002), 98 % relative humidity.

* Isotropic Young's modulus calculated for Poisson's ratio = 0.33.

Table 2. Best fit elastic constants of tetragonal hen egg-white lysozyme from measurements along the (110) plane. Bounds to C_{66} from mechanical stability constraints

Constant (GPa)	98% relative humidity	79% relative humidity	67% relative humidity
$C_{11} + C_{12} + 2C_{66}$	12.81 ± 0.08	20.4 ± 0.4	25.8 ± 0.8
C_{33}	5.48 ± 0.05	10.78 ± 0.09	13.62 ± 0.09
$C_{44} + 0.5C_{13}$	2.99 ± 0.05	5.19 ± 0.05	7.00 ± 0.05
C_{66}	$< 6.3^*$	$< 10.1^*$	$< 12.8^*$
χ^2_v	1.07 - 1.12	1.02 - 1.04	1.26 - 1.35
RMS (km/s)	0.012 - 0.013	0.011 - 0.012	0.017 - 0.018
K_S^{**}	0.12 - 5.44	0.29 - 10.1	0.27 - 13.8

$$\text{RMS (root mean square misfit)} = \sqrt{\sum_{i,1}^N (v_i^{obs} - v_i^{calc})^2 / N},$$

$$\chi^2_v \text{ (normalized } \chi^2) = \left[\sum_{i,1}^N \frac{(v_i^{obs} - v_i^{calc})^2}{\sigma_i^2} \right] / (N - m),$$

where N is the number of observations, v^{obs} and v^{calc} are the observed and calculated (model) velocities, σ is the uncertainty on the observed velocity, and m is the number of fitted parameters.

* Maximum value imposed by the mechanical stability requirements: $(C_{11} + C_{12})C_{33} - 2C_{13}^2 > 0$ and $C_{44} > 0$.

** Isostress (Reuss) bound to the calculated bulk modulus.

Table 3. Dynamic elastic constants of tetragonal hen egg-white lysozyme refined using additional Brillouin measurements along [100] direction and constraints from high-pressure x-ray diffraction

Constant (GPa)	98% relative humidity
C_{11}	5.49 ± 0.03
C_{12}	4.79 - 0.25
C_{13}	5.18 - 3.18
C_{33}	5.48 ± 0.05
C_{44}	$0.40 - 1.40^\dagger$
C_{66}	1.27 - 3.54
K_S^*	5.32 - 2.82
G^*	0.24 - 1.33
$E_{[110]}$	0.83 - 4.81
$E_{[001]}$	0.71 - 4.11

[†] Fixed value.

* Isostress bound to the modulus.

Figure captions

Figure 1. (a) Schematic diagram of the sample assemblages: (1) square cross-section glass capillary, for measurements in 180 and 90R scattering geometries, (2) sealed circular glass slides for measurements in the 90A forward geometry, V.P. vertical plane, H.P. horizontal plane; (b) – (e) diagrams of the scattering geometries in the different experimental configurations used in this study, k_0 incident wave vector, k_S scattered wave vector, q phonon wave vector, $\Delta\omega$ Brillouin scattering frequency shift, λ_0 incident laser wavelength, n refractive index of scattering medium, ω_0 incident frequency, ω_S scattered frequency.

Figure 2. Schematic diagram of the Brillouin scattering system.

Figure 3. A typical Brillouin spectrum collected from a crystal at 98% relative humidity.

The central elastic scattering peak (and its background) is scaled by a factor of 0.1.

Figure 4. Sound velocity of tetragonal lysozyme along the $[1\bar{1}0]$ and $[001]$ directions as a function of relative humidity. There is a discontinuous increase of both the velocities and an inversion of the velocity ratio corresponding to the 93% – 87% relative humidity range.

Figure 5. Elastic constant C_{33} , and the combinations $C_{11} + C_{12} + 2C_{66}$ and $C_{44} + 0.5C_{13}$ (see text) of tetragonal lysozyme plotted as a function of relative humidity.

Figure 6. Compressional sound velocities of tetragonal lysozyme crystals as a function of direction in the (110) plane. The solid lines are model velocities computed from the best fit elastic constants. Error bars are smaller than the symbols where not shown.

Figure 7. Range of values of the Young's moduli of lysozyme as determined using different techniques in different frequency ranges. See Table 1 for the data references.

Figure 8. Normalized phonon attenuation $\alpha\lambda_s$, as a function of relative humidity, calculated for phonons propagating along $[1\bar{1}0]$ and $[001]$ directions.

Figure 9. Contour plots of the root mean square (RMS) difference, expressed in km/s, between calculated and observed velocities along directions in the (110) plane of a crystal of tetragonal lysozyme at equilibrium hydration conditions (98% relative humidity). The RMS is plotted as a function of the two constants C_{13} and C_{44} while the values of $C_{11} + C_{12} + 2C_{66}$ and C_{33} are fixed to their best model values of 12.78 and 5.57 respectively. The shaded area represents a region in the constant space where the stability constraint: $(C_{11} + C_{12})C_{33} > 2C_{13}^2$ is violated.

Figure 10. Ranges of possible values of the elastic moduli of tetragonal lysozyme at 98% r.h. as a function of the value of the constant C_{44} . (a) Elastic constants and mechanical stability criteria (B_1 , B_2). (b) Aggregate Young's modulus ($E_{\text{Aggr.}}$), aggregate Poisson's ratio (σ), selected directional Young's moduli ($E_{[110]}$, $E_{[001]}$), and the isostress bound to the aggregate bulk (K_R) and shear (G_R) modulus.

$$B_1 = C_{11} - |C_{12}|$$

$$B_2 = (C_{11} + C_{12})C_{33} - 2C_{13}^2.$$

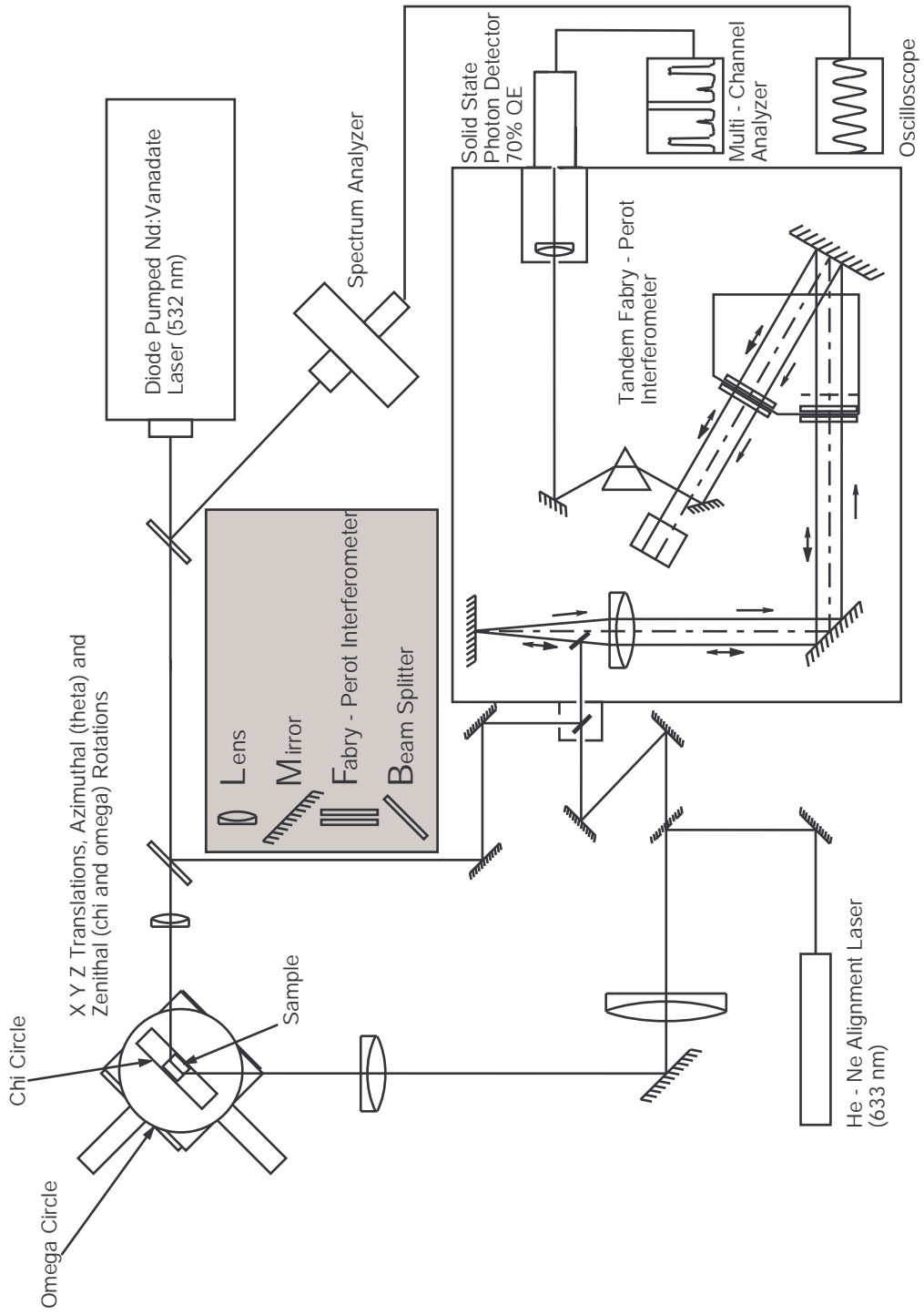


Figure 2

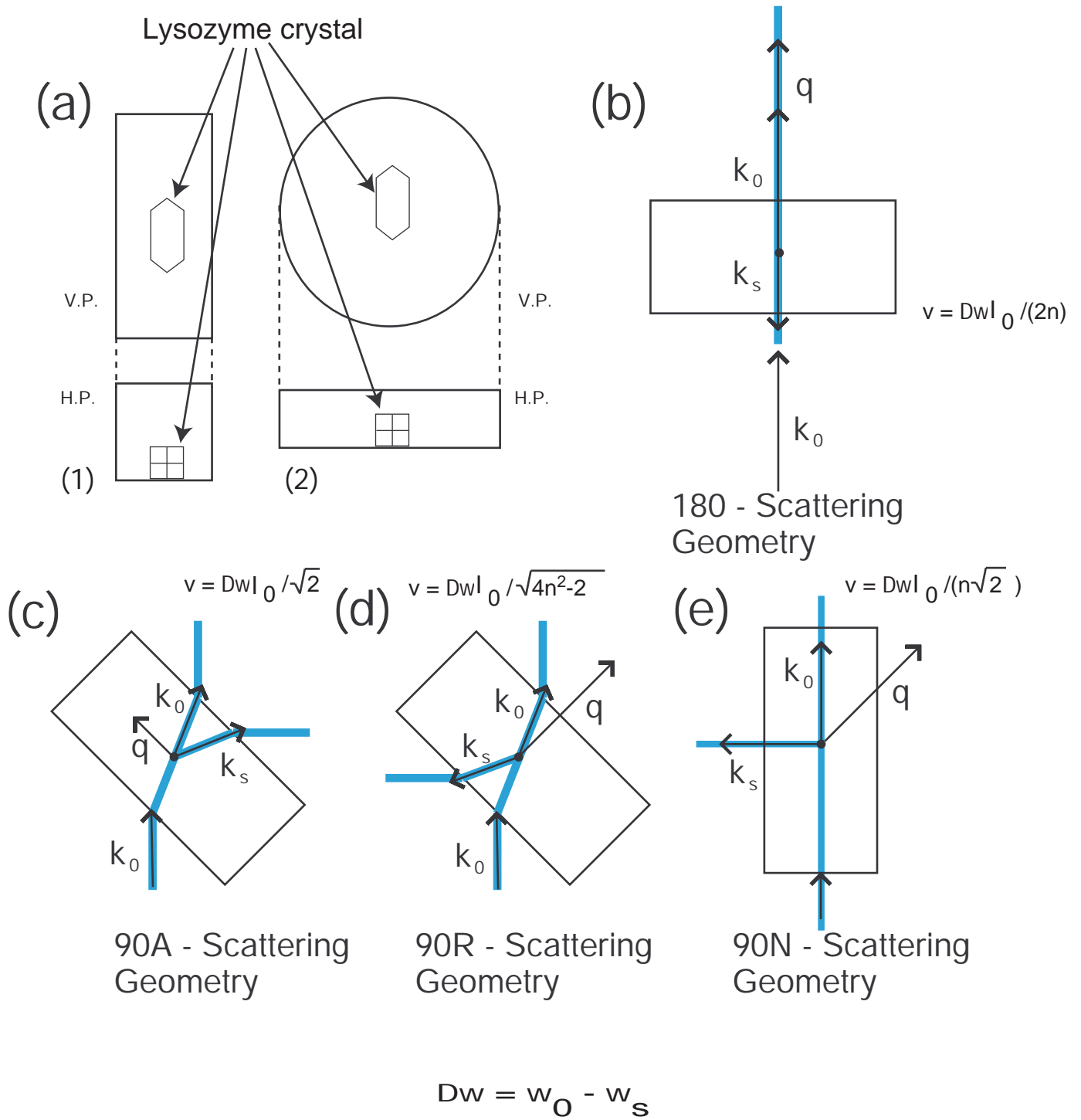


Figure 1

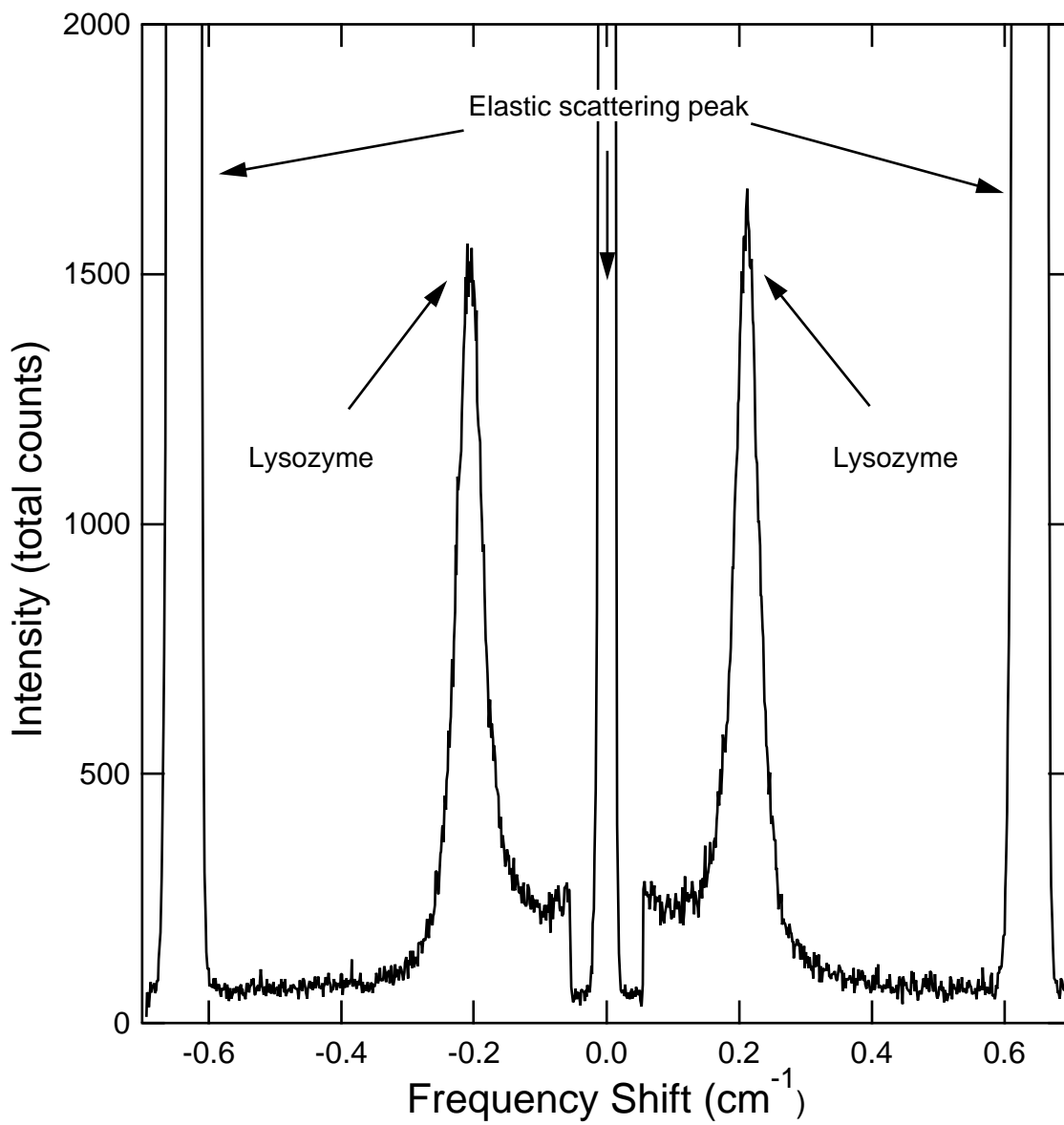


Figure 3

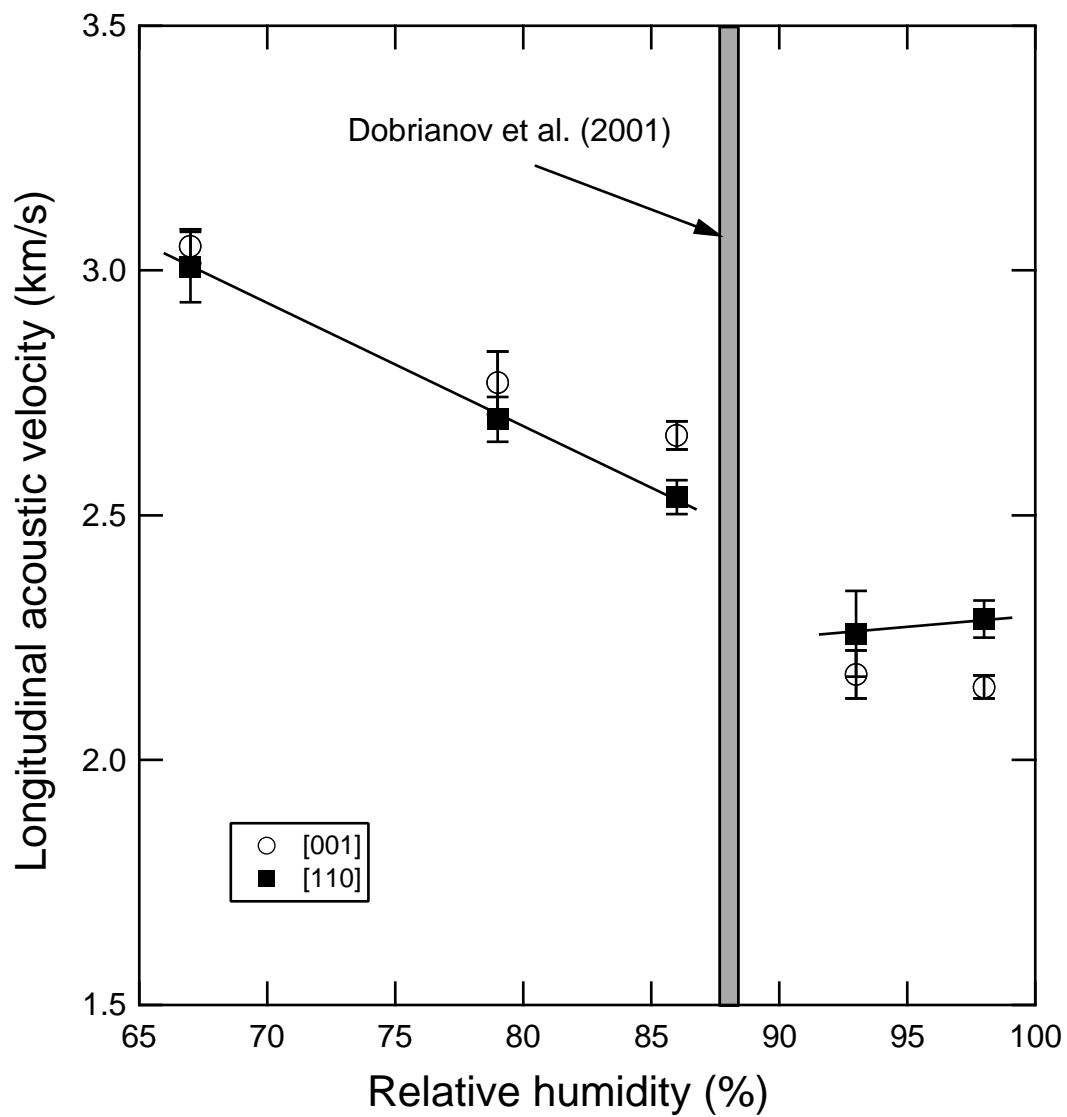


Figure 4

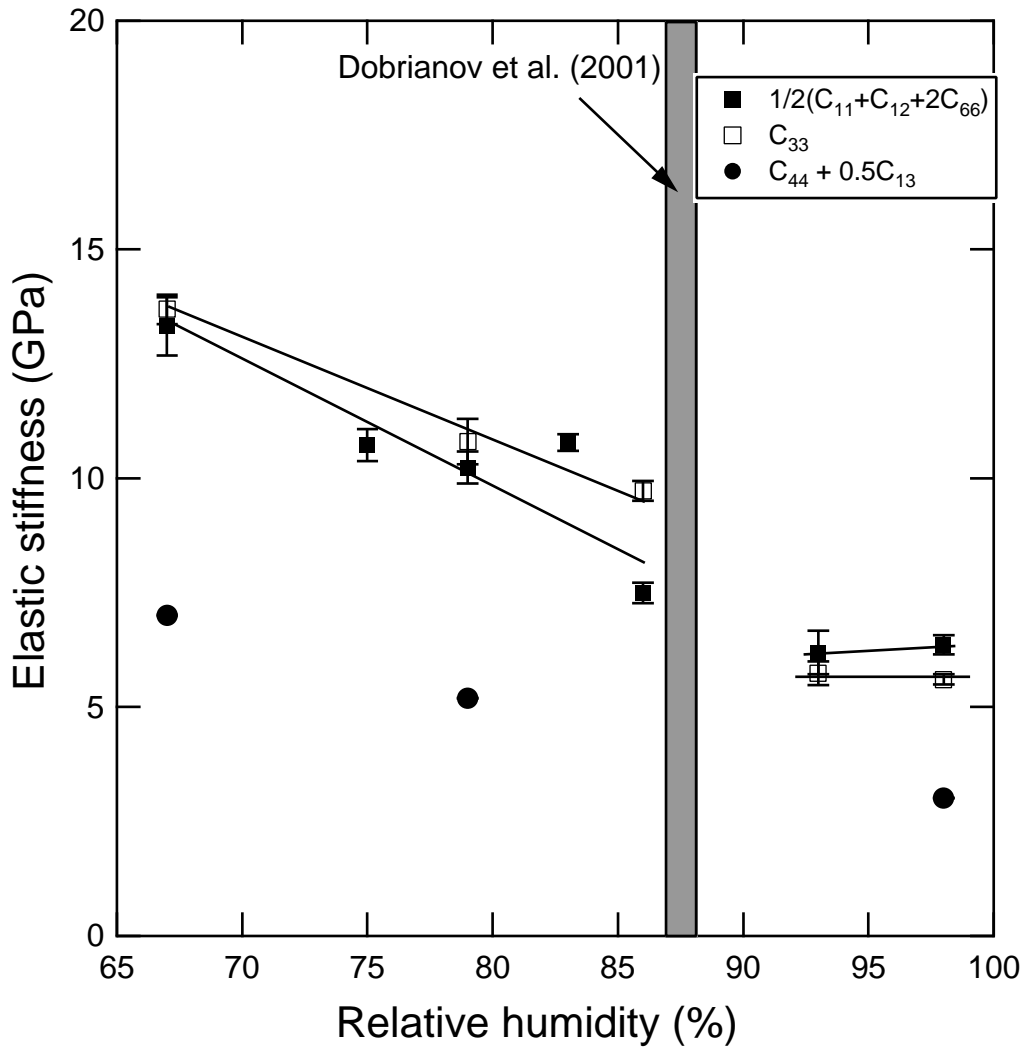


Figure 5

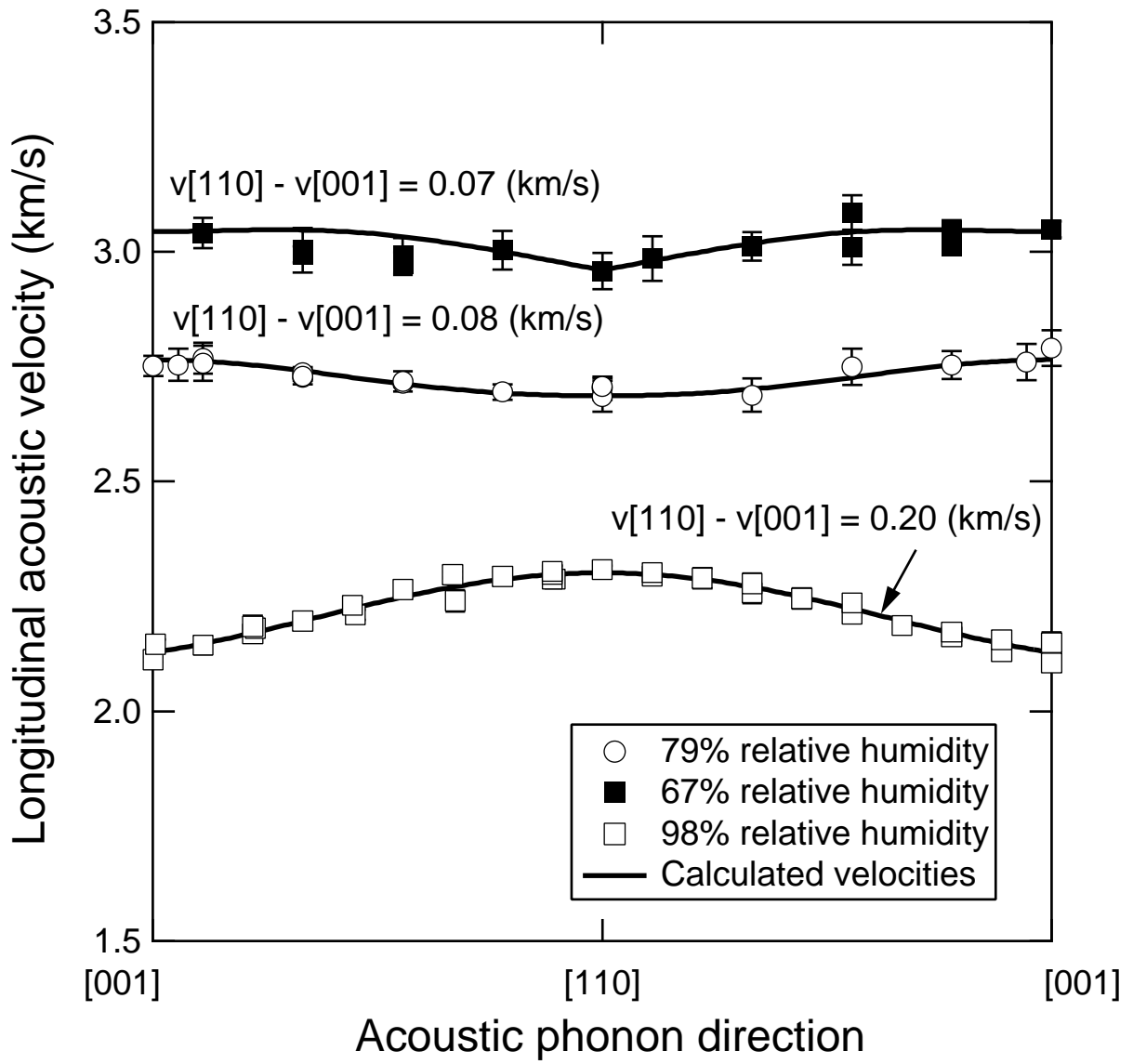


Figure 6

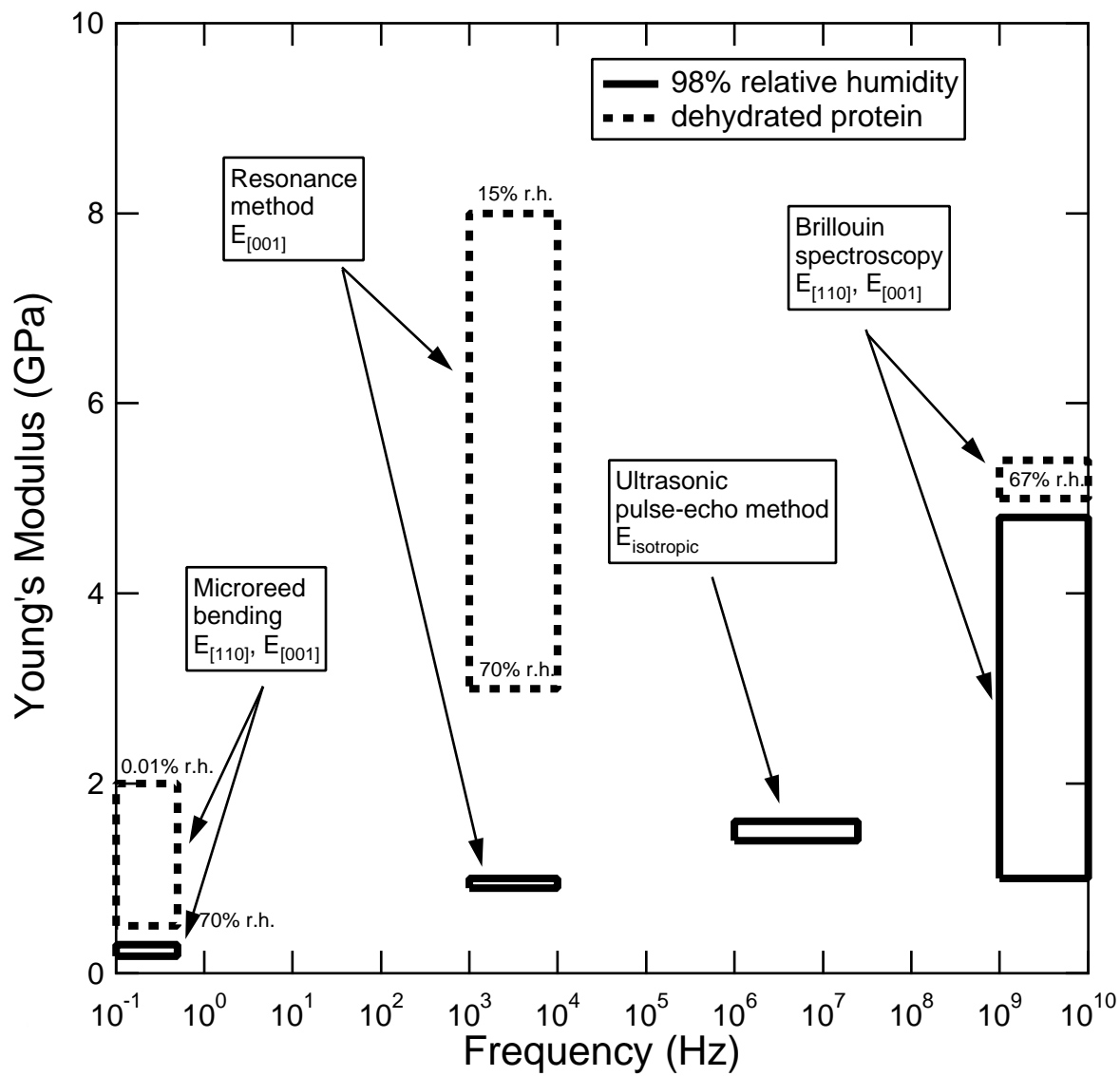


Figure 7

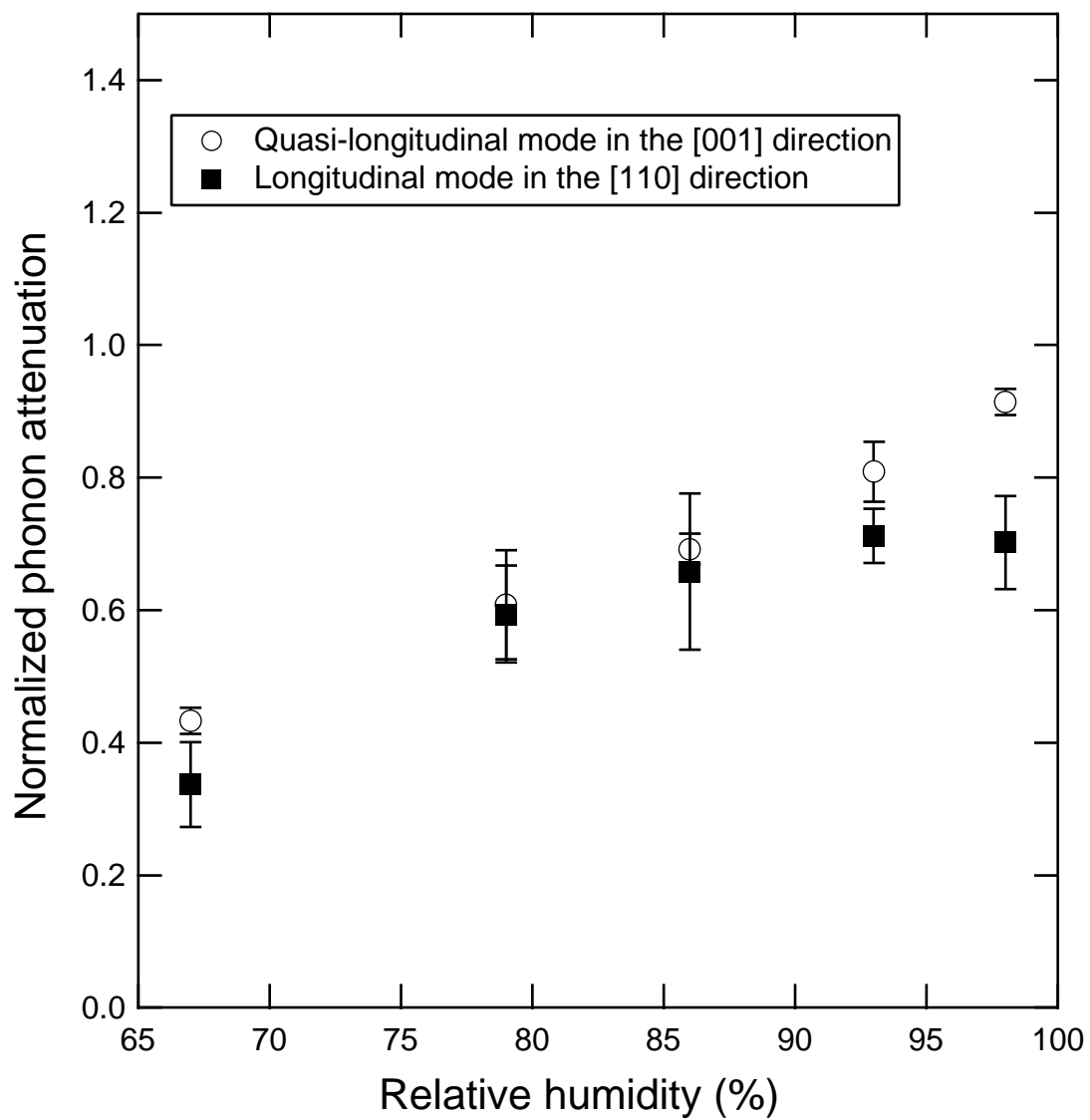


Figure 8

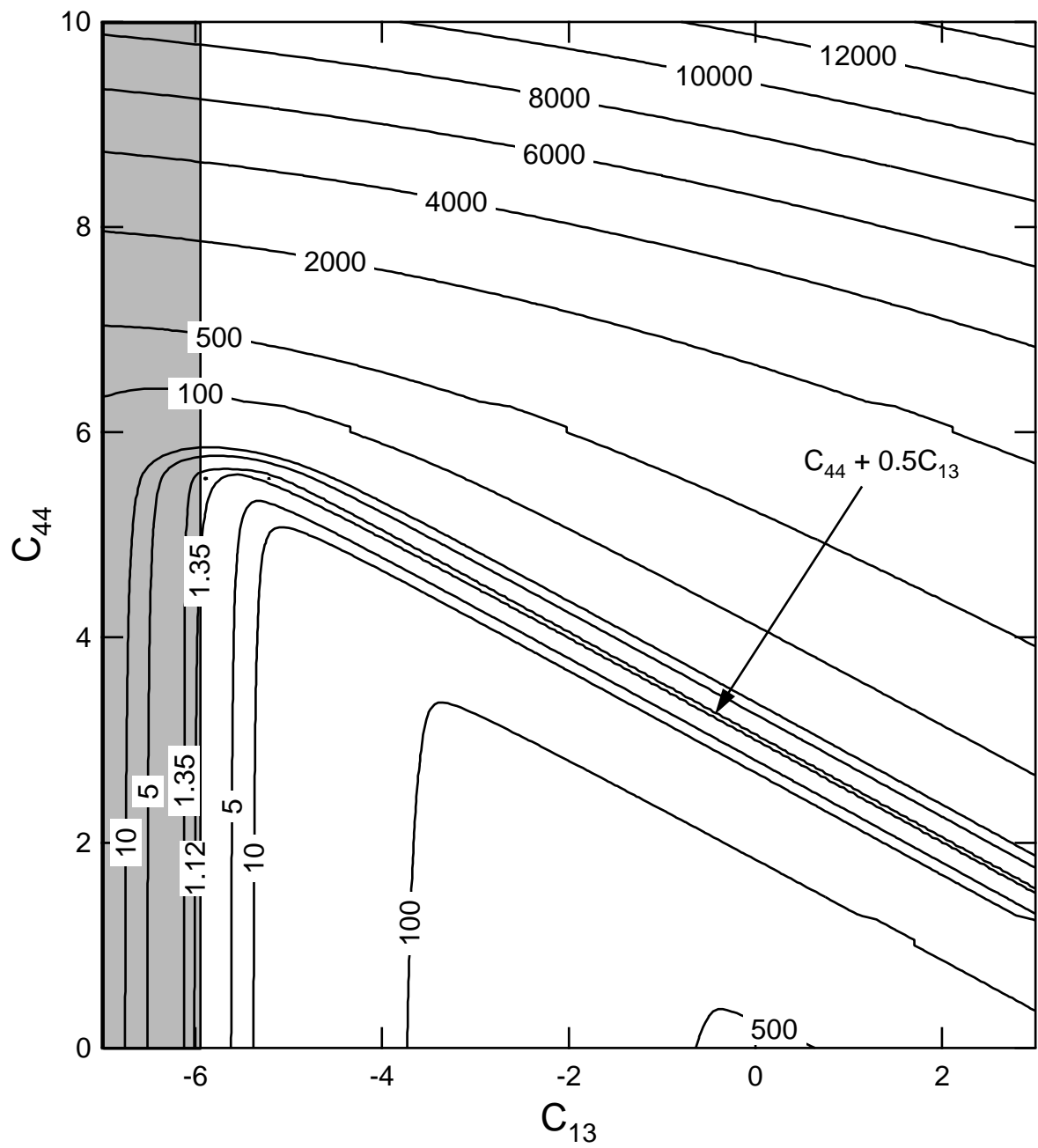


Figure 9

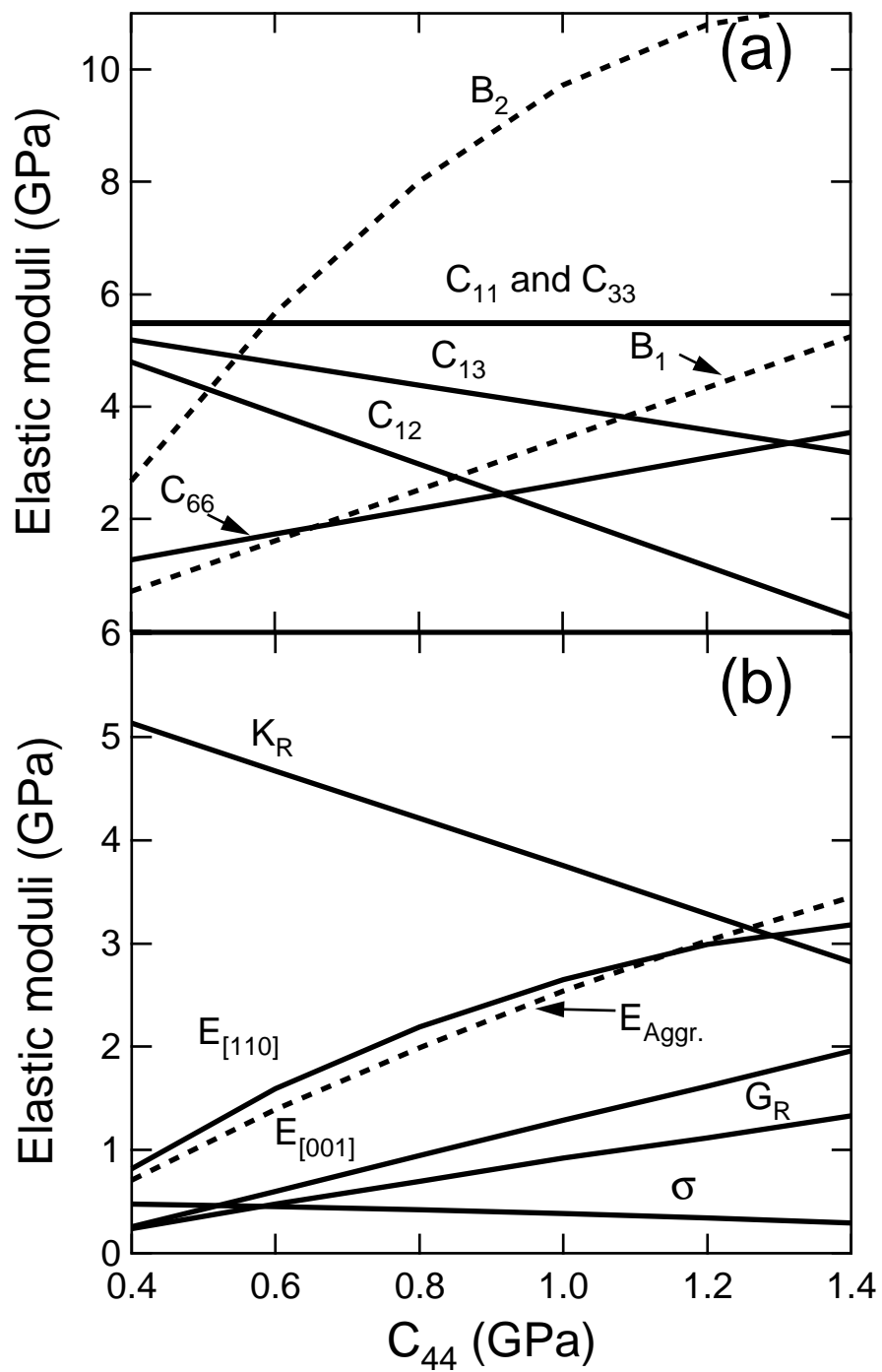


Figure 10